VIP Nanostructures Very Important Paper

Deutsche Ausgabe: DOI: 10.1002/ange.201501071
Internationale Ausgabe: DOI: 10.1002/anie.201501071

A Facile and Universal Top-Down Method for Preparation of Monodisperse Transition-Metal Dichalcogenide Nanodots**

*Xiao Zhang, Zhuangchai Lai, Zhengdong Liu, Chaoliang Tan, Ying Huang, Bing Li, Meiting Zhao, Linghai Xie, Wei Huang, and Hua Zhang**

Abstract: *Despite unique properties of layered transition-metal dichalcogenide (TMD) nanosheets, there is still lack of a facile and general strategy for the preparation of TMD nanodots (NDs). Reported herein is the preparation of a series of TMD NDs, including TMD quantum dots (e.g. MoS_2, WS_2, ReS_2, TaS_2, $MoSe_2$ and WSe_2) and $NbSe_2$ NDs, from their bulk crystals by using a combination of grinding and sonication techniques. These NDs could be easily separated from the N-methyl-2-pyrrolidone when post-treated with n-hexane and then chloroform. All the TMD NDs with sizes of less than 10 nm show a narrow size distribution with high dispersity in solution. As a proof-of-concept application, memory devices using TMD NDs, for example, $MoSe_2$, WS_2, or $NbSe_2$, mixed with polyvinylpyrrolidone as active layers, have been fabricated, which exhibit a nonvolatile write-once-read-many behavior. These high-quality TMD NDs should have various applications in optoelectronics, solar cells, catalysis, and biomedicine.*

Engineering the size and dimension of layered materials is one of the most fascinating ways to endow them with novel properties and broaden their applications. As a typical example, graphene quantum dots (QDs), one kind of nanodot (ND) with lateral sizes of less than 10 nm, exhibit extraordinary semiconducting properties and unique electrical/optical behaviors which are very different from those of gapless graphene nanosheets.[1] Therefore, it is believed that the preparation of other QDs of layered materials is fundamentally important and urgent since they are also expected to exhibit unusual properties and have promising applications.

Similar to graphene, single- or few-layer nanosheets of transition-metal dichalcogenides (TMDs), as a unique class of inorganic nanomaterials, showed various applications in electronics, catalysis, biomedicine, sensing, and energy storage.[2] Different from the conventional chalcogenide semiconductors, for example, CdS, PbS, and ZnS, TMDs with two-dimensional (2D) layered structures exhibit thickness-dependent physical properties.[2c] Recent work has mainly focused on the preparation of high-quality single- and few-layer TMD nanosheets, which exhibit dramatic changes in electronic and optical properties.[2c,e,3] Compared to the intrinsic 2D layers, the small-sized TMD semiconductors with a diameter of less than 10 nm, that is, TMD QDs, show stronger quantum confinement and edge effects, thus offering unique and extra electrical/optical properties beyond that of the single-/few-layer TMD nanosheets.[4] To date, most effort has been devoted to the exfoliation of 2D nanosheets.[2a,e,3a] Although sometimes the small-sized TMD nanostructures can be found during the preparation of 2D nanosheets, they are by-products with very low production yield.[5]

As known, monodispersed QDs synthesized in organic solvents using chemical methods,[6] that is, bottom-up methods, suffer from the insulating ligands coated on QDs, which are detrimental to the electrical transport, especially in the application of electronics[7] and catalysis.[7b,8] Alternatively, top-down approaches, such as laser ablation[9] and e-beam

[*] X. Zhang
Energy Research Institute @ NTU (ERI@N)
Interdisciplinary Graduate School
Nanyang Technological University
50 Nanyang Drive, Singapore 637553 (Singapore)
X. Zhang, Z. C. Lai, Z. D. Liu, C. L. Tan, Y. Huang, Dr. M. T. Zhao, Prof. H. Zhang
School of Materials Science and Engineering
Nanyang Technological University
50 Nanyang Avenue, Singapore 639798 (Singapore)
E-mail: hzhang@ntu.edu.sg
Homepage: http://www.ntu.edu.sg/home/hzhang/
Dr. B. Li
Institute of Materials Research and Engineering
Agency for Science, Technology and Research (A*STAR)
Singapore 117602 (Singapore)
Z. D. Liu, Prof. L. H. Xie, Prof. W. Huang
Key Laboratory for Organic Electronics and Information Display (KLOEID) and Institute of Advanced Materials (IAM), Jiangsu National Synergetic Innovation Center for Advanced Materials (SICAM)
Nanjing University of Posts and Telecommunications
9 Wenyuan Road, Nanjing 210046 (China)
Prof. W. Huang
Key Laboratory of Flexible Electronics (KLOFE) and Institute of Advanced Materials (IAM), Jiangsu National Synergistic Innovation Center for Advanced Materials (SICAM)
Nanjing Tech University (NanjingTech)
30 South Puzhu Road, Nanjing 211816 (China)

[**] This work was supported by MOE under AcRF Tier 2 (ARC 26/13, No. MOE2013-T2-1-034), AcRF Tier 1 (RG 61/12, RGT18/13, and RG5/13), and Start-Up Grant (M4080865.070.706022), and the Singapore Millennium Foundation in Singapore. This Research is also conducted by NTU-HUJ-BGU Nanomaterials for Energy and Water Management Programme under the Campus for Research Excellence and Technological Enterprise (CREATE), which is supported by the National Research Foundation, Prime Minister's Office, Singapore.

Supporting information for this article is available on the WWW under http://dx.doi.org/10.1002/anie.201501071.

lithography,[10] can be used to reduce the crystal size. Unfortunately, such methods are not feasible for the high-yield preparation of QDs in solution phase and are also restricted by the extremely expensive facilities. Up to now, the high-yield production of TMD QDs is still under investigation and their applications remain to be explored.

Herein, we report a general method, that is, a combination of a grinding and sonication process, to prepare a number of layered TMD NDs, including TMD QDs (e.g. MoS_2, WS_2, ReS_2, TaS_2, $MoSe_2$ and WSe_2) and $NbSe_2$ NDs, in high yield from the corresponding bulk TMD crystals at room temperature. All the prepared TMD NDs with sizes of less than 10 nm exhibit a narrow size distribution with high dispersity. As a proof-of-concept application, the synthesized TMD NDs, mixed with polyvinylpyrrolidone (PVP), are used as active layers for fabrication of memory devices with a non-volatile memory effect.

Layered TMDs in the form of MX_2 (M = transition metal and X = chalcogenide) are depicted by a planar covalently bound X-M-X sandwich structure. The basic structural characteristics of layered TMDs are displayed in Figure 1.

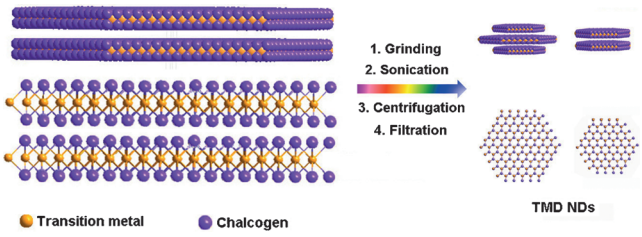

Figure 1. Preparation of TMD NDs from layered bulk TMDs.

Each single layer consists of two hexagonally close-packed chalcogenide atoms stacked with one close-packed transition-metal atom. Every two consecutive atomic layers stack through weak van der Waals interactions. To obtain small-sized TMD NDs, the in-plane X-M-X bonds should be broken. As known, grinding[11] and sonication[3a,12] are two typical processes to weaken the van der Waals interaction of TMDs, thus resulting in few-layer TMD nanosheets.[13] Moreover, the shear/compress force of grinding and the high-energy sonication are able to break up the covalent chemical bonds and disintegrate bulk crystals.[11,14] For example, recently, high-yield black phosphorus QDs have been successfully prepared from its bulk crystal in our group.[14a] Herein, $MoSe_2$ is used as a typical example to prove this method. The preparation process is shown in Figure 1. Briefly, $MoSe_2$ crystals were first ground with *N*-methyl-2-pyrrolidone (NMP) followed by sonication. The aforementioned process, grinding and then sonication, was repeated twice to improve the yield of $MoSe_2$ QDs and further decrease their size. The color of the original and resulting $MoSe_2$ suspensions is different, that is, it changed from black to dark brown (see Figure S1 in the Supporting Information), originating from their size difference.

After purification of the $MoSe_2$ suspension (Figure S1b), $MoSe_2$ QDs were obtained (see Experimental Section in the Supporting Information for details). The transmission electron microscopy (TEM) images showed that the size of $MoSe_2$ QDs are (2.7 ± 0.8) nm without aggregation (Figure 2a,b). High-resolution TEM (HRTEM) images of $MoSe_2$ QDs gave a clear lattice fringe of 0.21 nm deriving from the (104) planes

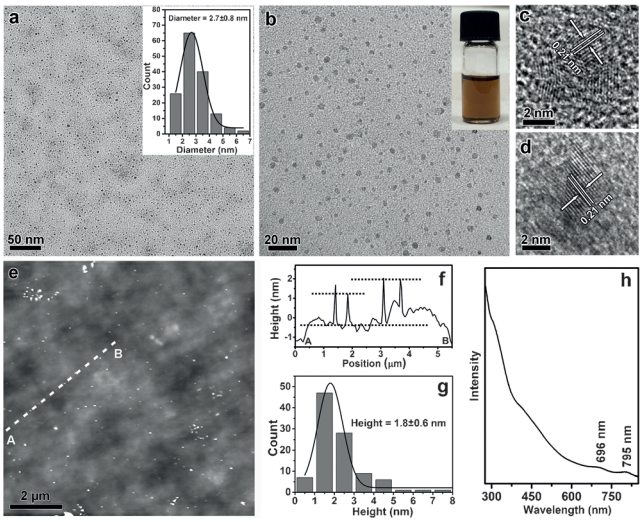

Figure 2. Characterization of $MoSe_2$ QDs. a) TEM image of $MoSe_2$ QDs. Inset in (a): Statistical analysis of the size of 150 $MoSe_2$ QDs measured from TEM images. b) Magnified TEM image of $MoSe_2$ QDs. Inset in (b): Photo of $MoSe_2$ suspension in NMP. c,d) HRTEM images of $MoSe_2$ QDs. e) AFM image of $MoSe_2$ QDs. f) Height profiles along the white dashed line in (e). g) Statistical analysis of the height of 100 $MoSe_2$ QDs measured from AFM images. h) UV-vis absorption spectrum of $MoSe_2$ QDs in NMP.

of the $MoSe_2$ crystal (Figure 2c,d), indicating the high crystallinity of the as-produced $MoSe_2$ QDs. Energy dispersive X-ray (EDX) analysis gave the signal of Mo, Se, and O (see Figure S2). Different from the black color of the original $MoSe_2$ suspension (see Figure S1a), the color of $MoSe_2$ QDs in NMP is brown (insert in Figure 2b). The chemical composition of $MoSe_2$ QDs was further confirmed with X-ray photoelectron spectroscopy (XPS). As shown in Figure S3, $MoSe_2$ QDs exhibited nearly the same binding energies for well-defined spin-coupled Mo and Se doublets as those of $MoSe_2$ crystal. The peaks around 228.8 and 232.0 eV correspond to Mo $3d_{5/2}$ and Mo $3d_{3/2}$, respectively (Figure S3a), while the peaks at 54.4 and 55.2 eV can be attributed to Se $3d_{5/2}$ and Se $3d_{3/2}$ orbitals, respectively (Figure S3b), which are in good agreement with the binding energies of Mo^{4+} and Se^{2-} in 2H phase of $MoSe_2$.[15] No obvious signal from the Mo^{6+} was observed, indicating that there is no obvious oxidation of $MoSe_2$ QDs. The atomic force microscopy (AFM) characterization confirmed that the height of the $MoSe_2$ QDs is (1.8 ± 0.6) nm (Figure 2e,f,g), that is, about 2 ± 1 layers, since the thickness of single-layer $MoSe_2$ is about 0.7 nm.[16] The optical property of the $MoSe_2$ QDs was measured by UV-vis absorption spectrum (Figure 2h). The characteristic excitonic peaks at $\lambda = 795$ nm (A) and 696 nm (B) are clearly observed, which arise from the direct transition from the valance band to the conduction

band at the K point of the Brillouin zoon,[17] indicating that the $MoSe_2$ QDs preserved the 2H-poly-type structure.[18]

Besides $MoSe_2$ QDs, our method has been successfully used to prepare a number of other TMD NDs, such as MoS_2, WS_2, ReS_2, TaS_2, WSe_2, and $NbSe_2$. The corresponding TEM and HRTEM images confirmed their high crystallinity and the diameters of the NDs are less than 10 nm (Figure 3).

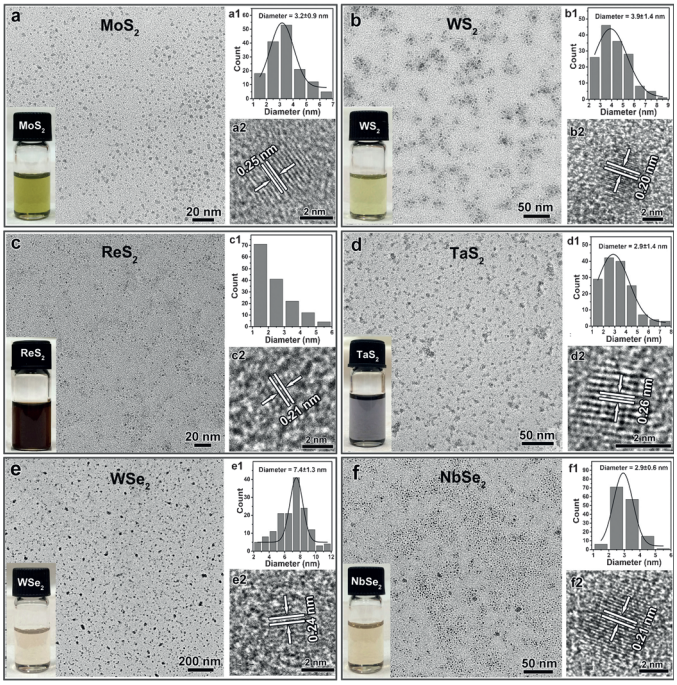

Figure 3. Characterization of other TMD NDs. a–f) TEM, HRTEM images and the size statistical analyses of MoS_2, WS_2, ReS_2, TaS_2, WSe_2, and $NbSe_2$ NDs. The corresponding photos of TMD NDs in NMP are inserted.

Specifically the thickness of typical MoS_2 QDs measured by AFM is (1.3 ± 0.7) nm (see Figure S4), that is, about 2 ± 1 layers, since the theoretical thickness of single-layer MoS_2 is about 0.65 nm. The obtained layer numbers of MoS_2 QDs are similar to those of $MoSe_2$ QDs. Because of the different light extinction coefficient, the prepared NDs displayed different colors in solution (see photographs in Figure 3; the corresponding UV-vis absorption spectra are shown in Figure S5).

Recently, Coleman et al. proved that NMP is one of the most effective solvents for exfoliation of TMDs because its surface energy matches that of TMD materials quite well, thus leading to the maximum dispersion of TMD nanosheets with high stability.[3a] However, the high dispersity and small size of NDs make it difficult to extract them from NMP, even using the high-speed centrifugation and/or solvent evaporation method. In this work, we report a simple method to realize the separation of NDs from NMP. After addition of *n*-hexane (poor solvent) and then chloroform (less polar solvent), the TMD ND dispersion can be easily precipitated through centrifugation (see Figure S6). The obtained products containing TMD NDs could be easily re-dispersed in other polar solvents, such as water and ethanol.

Previous studies have demonstrated that memory devices based on polymer–inorganic hybrids showed a unique conductance-switching effect and thus were regarded as the most promising alternative or supplementary devices for conventional inorganic semiconductor-based memory devices.[19] As a proof-of-concept application, the electronic properties and switching effects of PVP-$MoSe_2$ QD nanocomposite-based memory device with the configuration of glass/indium tin oxide (ITO)/PVP-$MoSe_2$ QDs/Au (inset in Figure 4a) was

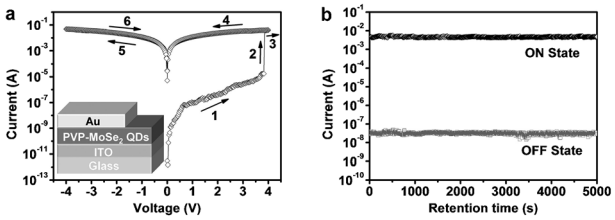

Figure 4. Memory device based on $MoSe_2$ QD. a) The *I–V* characteristics of this memory device. Inset in (a): The configuration of fabricated memory device. b) The retention-ability test of the memory device in the ON and OFF states at a reading voltage of $+0.5$ V.

fabricated and investigated by current-voltage (*I–V*) characteristics (see the Experimental Section in the Supporting Information for the detailed fabrication process of the device). As shown in Figure 4a, starting from the low conductivity state (OFF state) in the device (Stage 1), the current increased abruptly from 1.8×10^{-5} to 4.0×10^{-2} A with the applied positive voltage increasing to $+3.8$ V, indicating that the electrical property transformed from a low-current state (OFF state) into a high-current state (ON state; Stage 2). The transition from OFF to ON is equivalent to the "writing" process in a digital memory. In the subsequent positive sweep (Stages 3 and 4), the device remained in its high conductivity state with an ON/OFF ratio of over 4.0×10^5 at $+0.5$ V, which is significantly higher than that of PVP-MoS_2 nanosheet composite-based memory device.[20] This feature promises a low misreading rate during the device operation. After a reverse sweep to -4.0 V (Stage 5), the device remained at the high conductivity state (Stage 6), indicating the inerasable data-storage characteristic. Moreover, the high conductivity state persisted in subsequent sweeps (see Figure S7), suggesting the nonvolatile write-once-read-many (WORM) memory behavior of the device fabricated from a PVP-$MoSe_2$ QD nanocomposite.

For comparison, the *I–V* characteristics of a device with a configuration of Au/ITO/Au, without any active layer between ITO and Au, exhibited higher electrical conductivity compared to that of the memory device derived from a PVP-$MoSe_2$ QD nanocomposite after the electrical switching (see Figure S8), indicating that a short circuit did not occur during the operation of the device. To explore the stability of our device, the retention time test was carried out in the ON and OFF states, respectively (Figure 4b). The ON and OFF states of the device did not undergo significant fluctuation, even after more than 5.0×10^3 s of test at a reading bias of $+0.5$ V under ambient conditions. The long retention time demon-

strates the highly stable information storage capability of our device.

Moreover, under the same experimental conditions, devices based on PVP-WS_2 QD or PVP-$NbSe_2$ ND nanocomposites both exhibited the WORM memory effect (see Figures S9 and S10). The switching voltage of the device derived from PVP-WS_2 QD nanocomposite is at $+1.5$ V and the ON/OFF current ratio is over 1.7×10^3 at $+0.5$ V. For the device based on PVP-$NbSe_2$ ND nanocomposite, the transition from the OFF state to ON state occurred at a voltage of -1.3 V, and the ON/OFF current ratio is over 1.3×10^3 at -0.5 V. These two devices with low switching voltage reveal low writing voltage, suggesting promising applications in memory devices for low power consumption.

In summary, for the first time, we have systematically prepared the TMD NDs in high yield through a facile, universal top-down process. All the prepared NDs with diameters of less than 10 nm showed a narrow size distribution. As a proof-of-concept application, several types of NDs, that is, $MoSe_2$, WS_2, and $NbSe_2$, mixed with PVP were used as active layers for the fabrication of memory devices, which exhibited nonvolatile WORM memory effect with high ON/OFF current ratio. Among the tested devices, that derived from PVP-$MoSe_2$ QD nanocomposite showed the best performance with an ON/OFF ratio of over 4.0×10^5 and long-time stability. It is believed that the TMD NDs may have more promising applications in electronics, catalysis, solar cells, sensing, and biomedicine.

Keywords: memory devices · nanodots · quantum dots · transition metal dichalkogenides · two-dimensional materials

How to cite: *Angew. Chem. Int. Ed.* **2015**, *54*, 5425–5428
Angew. Chem. **2015**, *127*, 5515–5518

[1] a) S. Y. Lim, W. Shen, Z. Gao, *Chem. Soc. Rev.* **2015**, *44*, 362–381; b) K. A. Ritter, J. W. Lyding, *Nat. Mater.* **2009**, *8*, 235–242; c) Z. Zhang, J. Zhang, N. Chen, L. Qu, *Energy Environ. Sci.* **2012**, *5*, 8869–8869.

[2] a) X. Huang, Z. Zeng, H. Zhang, *Chem. Soc. Rev.* **2013**, *42*, 1934–1946; b) M. Chhowalla, H. S. Shin, G. Eda, L.-J. Li, K. P. Loh, H. Zhang, *Nat. Chem.* **2013**, *5*, 263–275; c) Q. H. Wang, K. Kalantar-Zadeh, A. Kis, J. N. Coleman, M. S. Strano, *Nat. Nanotechnol.* **2012**, *7*, 699–712; d) C. Tan, H. Zhang, *Chem. Soc. Rev.* **2015**, DOI: 10.1039/C4CS00182F; e) Z. Zeng, Z. Yin, X. Huang, H. Li, Q. He, G. Lu, F. Boey, H. Zhang, *Angew. Chem. Int. Ed.* **2011**, *50*, 11093–11097; *Angew. Chem.* **2011**, *123*, 11289–11293.

[3] a) J. N. Coleman, M. Lotya, A. O'Neill, S. D. Bergin, P. J. King, U. Khan, K. Young, A. Gaucher, S. De, R. J. Smith, I. V. Shvets, S. K. Arora, G. Stanton, H. Y. Kim, K. Lee, G. T. Kim, G. S. Duesberg, T. Hallam, J. J. Boland, J. J. Wang, J. F. Donegan, J. C. Grunlan, G. Moriarty, A. Shmeliov, R. J. Nicholls, J. M. Perkins, E. M. Grieveson, K. Theuwissen, D. W. McComb, P. D. Nellist, V. Nicolosi, *Science* **2011**, *331*, 568–571; b) G. Eda, H. Yamaguchi, D. Voiry, T. Fujita, M. W. Chen, M. Chhowalla, *Nano Lett.* **2011**, *11*, 5111–5116.

[4] a) H. D. Ha, D. J. Han, J. S. Choi, M. Park, T. S. Seo, *Small* **2014**, *10*, 3858–3862; b) H. Huang, C. Du, H. Shi, X. Feng, J. Li, Y. Tan, W. Song, *Part. Part. Syst. Char.* **2015**, *32*, 72–79; c) L. Lin, Y. Xu, S. Zhang, I. M. Ross, A. C. M. Ong, D. A. Allwood, *ACS Nano* **2013**, *7*, 8214–8223.

[5] a) D. Gopalakrishnan, D. Damien, M. M. Shaijumon, *ACS Nano* **2014**, *8*, 5297–5303; b) J.-Y. Wu, M.-N. Lin, L.-D. Wang, T. Zhang, *J. Nanomater.* **2014**, *2014*, 7.

[6] V. Lesnyak, N. Gaponik, A. Eychmuller, *Chem. Soc. Rev.* **2013**, *42*, 2905–2929.

[7] a) G. Konstantatos, I. Howard, A. Fischer, S. Hoogland, J. Clifford, E. Klem, L. Levina, E. H. Sargent, *Nature* **2006**, *442*, 180–183; b) H. Zhang, B. Hu, L. Sun, R. Hovden, F. W. Wise, D. A. Muller, R. D. Robinson, *Nano Lett.* **2011**, *11*, 5356–5361.

[8] B. H. Kim, M. J. Hackett, J. Park, T. Hyeon, *Chem. Mater.* **2014**, *26*, 59–71.

[9] Y.-P. Sun, B. Zhou, Y. Lin, W. Wang, K. A. S. Fernando, P. Pathak, M. J. Meziani, B. A. Harruff, X. Wang, H. Wang, P. G. Luo, H. Yang, M. E. Kose, B. Chen, L. M. Veca, S.-Y. Xie, *J. Am. Chem. Soc.* **2006**, *128*, 7756–7757.

[10] L. A. Ponomarenko, F. Schedin, M. I. Katsnelson, R. Yang, E. W. Hill, K. S. Novoselov, A. K. Geim, *Science* **2008**, *320*, 356–358.

[11] I.-Y. Jeon, Y.-R. Shin, G.-J. Sohn, H.-J. Choi, S.-Y. Bae, J. Mahmood, S.-M. Jung, J.-M. Seo, M.-J. Kim, D. Wook Chang, L. Dai, J.-B. Baek, *Proc. Natl. Acad. Sci. USA* **2012**, *109*, 5588–5593.

[12] V. Nicolosi, M. Chhowalla, M. G. Kanatzidis, M. S. Strano, J. N. Coleman, *Science* **2013**, *340*, 1226419.

[13] Y. G. Yao, L. Tolentino, Z. Z. Yang, X. J. Song, W. Zhang, Y. S. Chen, C. P. Wong, *Adv. Funct. Mater.* **2013**, *23*, 3577–3583.

[14] a) X. Zhang, H. Xie, Z. Liu, C. Tan, Z. Luo, H. Li, J. Lin, L. Sun, Z. Xu, W. Chen, L. Xie, W. Huang, H. Zhang, *Angew. Chem. Int. Ed.* **2015**, DOI: 10.1002/anie.201409400; *Angew. Chem.* **2015**, DOI: 10.1002/ange.201409400; b) X. Zhou, S. Guo, J. Zhang, *ChemPhysChem* **2013**, *14*, 2627–2640.

[15] a) H. Wang, D. Kong, P. Johanes, J. J. Cha, G. Zheng, K. Yan, N. Liu, Y. Cui, *Nano Lett.* **2013**, *13*, 3426–3433; b) H. Tang, K. Dou, C.-C. Kaun, Q. Kuang, S. Yang, *J. Mater. Chem. A* **2014**, *2*, 360–364.

[16] G. W. Shim, K. Yoo, S.-B. Seo, J. Shin, D. Y. Jung, I.-S. Kang, C. W. Ahn, B. J. Cho, S.-Y. Choi, *ACS Nano* **2014**, *8*, 6655–6662.

[17] K. Wang, Y. Feng, C. Chang, J. Zhan, C. Wang, Q. Zhao, J. N. Coleman, L. Zhang, W. J. Blau, J. Wang, *Nanoscale* **2014**, *6*, 10530–10535.

[18] a) A. R. Beal, J. C. Knights, W. Y. Liang, *J. Phys. C* **1972**, *5*, 3540; b) J. A. Wilson, A. D. Yoffe, *Adv. Phys.* **1969**, *18*, 193–335.

[19] a) J.-S. Lee, J. Cho, C. Lee, I. Kim, J. Park, Y.-M. Kim, H. Shin, J. Lee, F. Caruso, *Nat. Nanotechnol.* **2007**, *2*, 790–795; b) W.-P. Lin, S.-J. Liu, T. Gong, Q. Zhao, W. Huang, *Adv. Mater.* **2014**, *26*, 570–606; c) J. Ouyang, C.-W. Chu, C. R. Szmanda, L. Ma, Y. Yang, *Nat. Mater.* **2004**, *3*, 918–922.

[20] J. Liu, Z. Zeng, X. Cao, G. Lu, L.-H. Wang, Q.-L. Fan, W. Huang, H. Zhang, *Small* **2012**, *8*, 3517–3522.

Received: February 4, 2015
Published online: March 11, 2015

